Journal of Sound and Vibration 329 (2010) 5005–5016

Contents lists available at ScienceDirect

Journal of Sound and Vibration

journal homepage: www.elsevier.com/locate/jsvi

Adaptive nonlinear neuro-controller with an integrated evaluation algorithm for nonlinear active noise systems ☆

Xinghua Zhang, Xuemei Ren *, Jing Na, Bo Zhang, Hong Huang

School of Automation, Beijing Institute of Technology, Beijing 100081, China

ARTICLE INFO

Article history:
Received 11 August 2009
Received in revised form
27 April 2010
Accepted 21 June 2010
Handling Editor: J. Lam
Available online 15 July 2010

ABSTRACT

An adaptive nonlinear neuro-controller with an integrated evaluation algorithm for nonlinear active noise control systems is proposed to attenuate the nonlinear and non-Gaussian noises. Inspired by the structure of the Hammerstein or Wiener model, the proposed controller is realized by the static nonlinear memory function mapping on the basis of a single neuron. A generalized filtered-X gradient descent algorithm based on an integrated evaluation criterion is developed to adaptively adjust the weights of the controller, where the weighted sum of Renyi's quadratic error entropy and the mean square error is applied as the integrated performance index, which improves the performance of the adaptive algorithm by introducing the information entropy. In addition, the convergence of the proposed approach is analyzed, and the computational complexity among different methods is investigated. The proposed scheme can effectively attenuate the nonlinear and non-Gaussian noises and has a relative simple structure and less learning parameters. The simulation results demonstrate the validity of the proposed method for attenuating the nonlinear and non-Gaussian noises.

1. Introduction

Noise control has been widely studied in the past decades. Active noise control (ANC) technology has been of great attention due to the development of adaptive control algorithm and the advancement of digital signal processors. ANC is based on the principle that a noise can be canceled by generating another noise with the same amplitude but an opposite phase. Comparing with the traditional passive noise control, ANC has potential benefits in size, weight, and cost, and especially which is an available method for noise suppression in low frequency ranges [1]. Based on a linear finite-impulse-response (FIR) filter structure, the filtered-X least mean square (FXLMS) algorithm and the modified schemes [1–5] using the mean square error criterion, have been successfully used for linear ANC systems due to their simplicity in design, robustness, and relatively low computational load. Those linear ANC methods have been widely applied into aircraft engineers, automobile, heating, air conditioning duct systems, and others [1–3]. However, in the practical ANC systems, nonlinearities may degrade the performance of linear ANC methods [6]. In fact, the primary and the secondary path of the ANC system may exhibit nonlinear behaviors, and the noises injected into a dynamic system may be highly nonlinear and non-Gaussian signals, which render linear ANC methods not suitable for nonlinear ANC systems [7]. In [8], an adaptive Volterra filter was introduced for feedforward ANC system, and a Volterra filtered-X LMS (VFX-LMS) algorithm was

☆ This work was supported by the National Natural Science Foundation of China under Grant no. 60974046.

* Corresponding author. Tel.: +86 1068914506.
E-mail addresses: xhzbird@bit.edu.cn (X. Zhang), xmren@bit.edu.cn (X. Ren), najing2120002@yahoo.com.cn (J. Na), zhangbo@bit.edu.cn (B. Zhang), honghuang@bit.edu.cn (H. Huang).

0022-460X/$ - see front matter © 2010 Elsevier Ltd. All rights reserved.
doi:10.1016/j.jsv.2010.06.017

proposed for nonlinear noises. The major disadvantage of using a Volterra filter is that the computational complexity increases exponentially as the order of the input increases. In recent years, multilayer perception networks [9–11], radial basis function networks [12,13], and recurrent fuzzy neural networks [14] have also been introduced to control the nonlinear noise process. In [6], the filtered-S LMS (FSLMS) algorithm has been proposed to deal with the nonlinear problem based on the functional link neural networks (FLNNs). Adaptive feedback FLNN filter with a reduced complexity FSLMS algorithm [15] has been proposed for active control of nonlinear noise processes. In [7], a general nonlinear filter with filtered-error expansion was used to solve the nonlinear ANC problem. Although the nonlinear control methods aforementioned [6,7,9–14] can achieve better performance for noise attenuation, they are with the more complicated structures and are difficult to implement in the practical system compared to the Volterra filter.

The least mean square (LMS) algorithm has been applied as a popular approach for the ANC systems, which is based on the mean square error (MSE) criterion. Nevertheless, the MSE criterion only considers the second-order statistics information of signals, and neglects real subsistent non-Gaussian information. Under the circumstances of nonlinear and non-Gaussian noises, the methods based on the MSE criterion cannot extract all possible information from the signals. Therefore the algorithms with the MSE criterion cannot perform well for the control systems including the non-Gaussian noises [16]. Since Shannon introduced the term named Information Theory, and defined information entropy (IE) as a precise mathematical measure of information uncertainty, the information theoretic approaches have been paid more and more attentions in the field of adaptive signal processing and control areas [14–22]. IE can provide a more comprehensive description of signals, this is, IE can include all possible higher order information of a random variable under the condition of nonlinearity and non-Gaussian. In recent years, some algorithms based on IE have been proposed in the field of independent component analysis [17], blind source separation [18], and non-Gaussian stochastic control systems [16,19,20].

Based on the above considerations, this paper introduces the information theory into the nonlinear and non-Gaussian noise control systems, and proposes a novel active noise controller which is extended by the nonlinear memory function mapping on the basis of a single neuron. Inspired by the structure of Hammerstein or Wiener Model [23–28], a new structure of adaptive controller is proposed, which includes a static nonlinear memory function mapping part and a dynamic neuron part. The static nonlinear memory function mapping is realized by a nonlinear function mapping and a memory group in order to form the generalized input of the dynamic linear part, where the nonlinear function mapping is implemented through a static input to obtain a P order signal sequence, and the memory group preserves $N-1$ the historical input elements. Then the dynamic linear part is used to conduct the weights adjustment using a single neuron structure. Consequently, this controller has a simpler structure and less learning parameters compared with the nonlinear ANC methods mentioned above [8–15], especially a Volterra filter.

In addition, a generalized filtered-X integrated-evaluation-criterion-based gradient descent (GFX-IECGD) algorithm is presented for the proposed controller in this paper. Considering the fact that MSE criterion has a good sensitivity to the mean value of the error sample, a weighted sum of Renyi's quadratic error entropy and the mean square error is defined as the integrated evaluation criterion, which can improve the performance of IE criterion and avoid the possible constant steady-state tracking error in the systems [20]. The probability density function of the system error is estimated by the Parzen-window estimation method [29]. Furthermore, the convergence of the proposed approach is analyzed, and the computational complexity among several different methods is discussed.

This paper is organized as follows. Section 2 describes a nonlinear ANC system. Section 3 presents the nonlinear neuro-controller with GFX-IECGD algorithm. In Section 4 the convergence and the self-adjustment process of the proposed approach is discussed. In Section 5 the computational complexity is studied. The simulation results are given in Section 6. Finally, conclusions are summarized in Section 7.

2. Nonlinear ANC systems

In the feedforward ANC system [1], the noise from the noise source is spread in the primary path (e.g., duct), and the feedforward superposition signal with the same amplitude but an opposite phase is generated by a controller. The performance of noise attenuation is measured by an error sensor at the noise cancelation point. The noise system may be time-varying because of the characteristics of noise source and the time-variability of the environment, thus it is necessary to design an adaptive noise controller generating a secondary noise source. An ANC system with a nonlinear primary noise path and a linear secondary noise path is shown in Fig. 1, where the secondary path is with a known model, which can be estimated off-line with a FIR filter [1,2].

In Fig. 1, $P(z)$ is the primary path transfer function from the reference signal $x(k)$ to the error signal $e(k)$ at the noise cancelation point, which defines the dynamics from the noise source to the error sensor. $S(z)$ is the secondary path transfer function from the output $u(k)$ of a nonlinear controller to $e(k)$, which includes a D/A converter, an amplifier, and an actuator (this is usually an audio loudspeaker), the path from the loudspeaker to the error sensor, and the electro-acoustic response of the error sensor. The transfer function $S(z)$ can be estimated off-line by an adaptive FIR filter $\hat{S}(z)$. $d(k)$ is the primary noise to be canceled at the error sensor, $y(k)$ is the secondary noise at the noise cancelation point. The error $e(k)$ of the nonlinear ANC system can be described as

$$e(k) = d(k) - y(k) = g(x(k)) - s(k) * u(k) \tag{1}$$

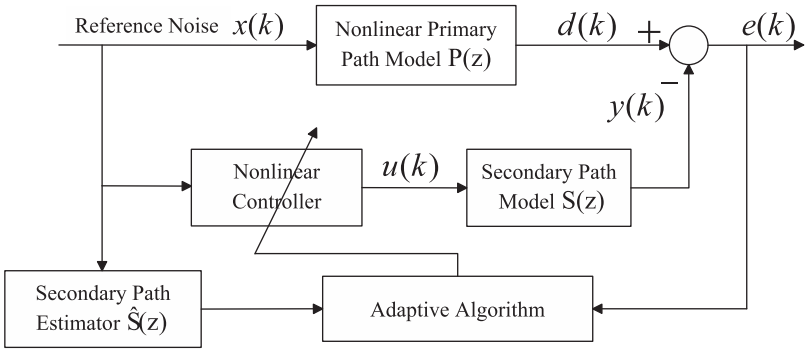

Fig. 1. Nonlinear feedforward active noise control systems.

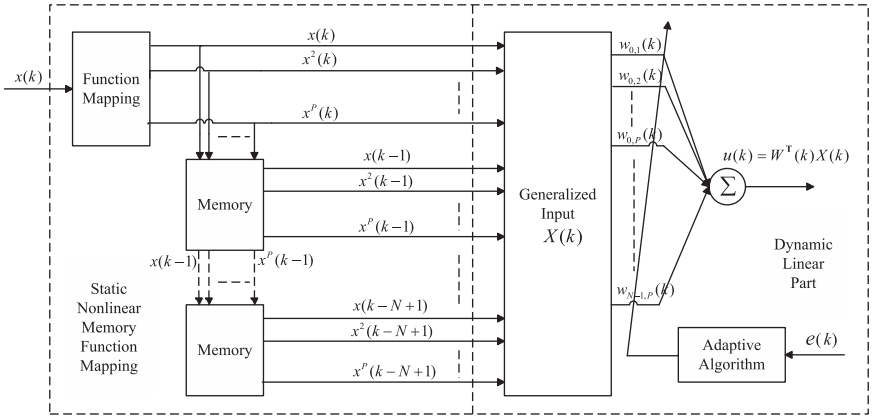

Fig. 2. Block diagram of adaptive nonlinear neuro-controller.

where $x(k)$ is the reference noise signal, $g(\cdot)$ is a smooth nonlinear function which represents the nonlinear primary noise path, $u(k)$ is the output of the nonlinear controller, $s(k)$ is the impulse response of the secondary path model $S(z)$, and the operator $*$ denotes the linear convolution.

The output of the feedforward nonlinear controller can be expressed as

$$u(k)=f(W(k),x(k)) \tag{2}$$

where $f(\cdot)$ is a generalized smooth nonlinear function, which represents the proposed nonlinear neuro-controller shown in Fig. 2. $W(k)$ is the generalized weight coefficient vector of the proposed nonlinear controller. The purpose of this paper is to design active noise controller with an algorithm to attenuate the nonlinear and non-Gaussian noises.

3. Adaptive nonlinear neuro-controller with an integrated evaluation algorithm

3.1. Nonlinear neuro-controller

Neural networks (NNs) have been applied to nonlinear systems for many years [30]. Some controllers based on NNs [6,7,9–15] have also been introduced to control the nonlinear noise process. The control methods mentioned above use the networks with hidden layers, which are the extended styles on the basis of a single neuron, and those controllers are with complicated structures, heavy computational burden, and even slow convergence. Inspired by the structure of Hammerstein or Wiener model, we propose a structure of controller based on a simple single neuron, which is a special NN. However, the proposed controller only needs to adaptively adjust the weights of the dynamic linear part with a single neuron.

As known, Hammerstein or Wiener model is a representation of nonlinearity [23], which has been applied to system identification [24–26] and predictive control based on identification model [27,28]. Inspired by the structure of Hammerstein or Wiener model, an adaptive ANC controller shown in Fig. 2 is developed, which includes a static nonlinear memory part and a dynamic linear part. The static nonlinear memory part is realized by a nonlinear function mapping which is a nonlinear extension, and a memory group which is used to preserve the historical information. In addition, the dynamic linear part is a single neuron with unknown weights adaptively updated by an algorithm given in Section 3.2.

In Fig. 2, the input $x(k)$ is extended into a vector $X'(k)=[x(k),x^2(k),\ldots,x^P(k)]\in R^P$ through the static function mapping, this extension can make the proposed method to deal with the nonlinear noise well, and the memory as shown in Fig. 2 preserves the vector $X'(k)$, with $N-1$ output sequences, this is, $X'(k-1),X'(k-2),\ldots,X'(k-N+1)$. Therefore, the generalized input $X(k)\in R^{NP}$ of the dynamic linear part contains NP elements, this is, $X(k)=[X'(k),X'(k-1),\ldots,X'(k-N+1)]^{\mathrm{T}}$, $X'(k-i)=[x(k-i),x^2(k-i),\ldots,x^P(k-i)]^{\mathrm{T}}$, $i=0,1,\ldots,N-1$.

As shown in Fig. 2, the dynamic linear part is realized by a single neuron, which has one output $u(k)$. The output of the proposed controller is given through a single neuron. The output of the proposed controller is expressed as

$$u(k)=W^{\mathrm{T}}(k)X(k) \tag{3}$$

where $W(k)\in R^{NP}$ is the generalized weight coefficient of the dynamic neuron part described by a $NP\times 1$ vector. The error signal is described as $e(k)=d(k)-y(k)$, which is the output of the noise sensor at the noise cancelation point.

Remark 1. Compared to the Volterra filter [8], the proposed controller can be regarded as a simplified case of a Volterra filter since it decreases the dimension of input of a Volterra filter. In addition, the proposed neuro-controller has a simple structure since it does not need to design the hidden layer and activation function. However, it can be considered as a special NN since a single neuron is applied to realize the performance of the whole adaptive controller.

3.2. GFX-IECGD algorithm

The MSE criterion has been applied to train adaptive linear filters and neural networks as the fundamental performance index. However, MSE criterion merely considers the second-order statistic, thus it cannot satisfy the control demand for non-Gaussian noises. Information entropy (IE) can provide a general description of system with non-Gaussian noises compared with the mean or variance. However, IE is merely a variation degree of the variable, and it does not consider the mean value information [21]. In viewing the fact that the MSE criterion has a good sensitivity to the mean of random variable, which can handle the shortcoming of IE. Therefore, a generalized filtered-X integrated-evaluation-criterion-based gradient descent (GFX-IECGD) algorithm is proposed in this section.

The integrated performance index of the error e can be defined as

$$J=\eta E(e^2)-(1-\eta)\log\left(\int f^2(e)\,\mathrm{d}e\right) \tag{4}$$

where the first term in the right of Eq. (4) represents the index of the MSE, and the second term is the index of Renyi's quadratic error entropy, η is the weighted factor, $0\le\eta\le 1$, and $f(e)$ represents the probability density function (PDF) of the system error e, E is the expectation operator. Among the different entropy measure definitions, Renyi's quadratic entropy has the advantage of computational efficiency compared to others [17], and is utilized in this paper.

Remark 2. The selection of the weighted factor η depends on the practical system. It should be chosen as a tradeoff between the steady-state error and noise attenuation. In general, its choice is a compromise: a big η yields a small MSE of system error e, but will perform worse for the non-Gaussian noises. However, a small η can attenuate the non-Gaussian noises, but may exist a constant error e in the system.

From Eq. (4), the integrated performance index of error $e(k)$ at time k can be expressed as

$$\begin{aligned}J&=\eta E(e^2(k))-(1-\eta)\log\left(\int f^2(e(k))\,\mathrm{d}e\right)\\&=\eta E(e^2(k))-(1-\eta)\log\left(\int f(e(k))f(e(k))\,\mathrm{d}e\right)\\&=\eta E(e^2(k))-(1-\eta)\log(E\{f(e(k))\})\end{aligned} \tag{5}$$

For reducing the computational complexity of the algorithm, $E\{f(e(k))\}$ and $E(e^2(k))$ can be replaced by their instantaneous values $f(e(k))$ and $e^2(k)$, respectively [17], then we can rewrite Eq. (5) as follows:

$$J=\eta e^2(k)-(1-\eta)\log(f(e(k))) \tag{6}$$

In order to minimize the index of Eq. (6), according to the gradient descent algorithm, the generalized weight coefficient $W(k)$ in Fig. 2 is updated as

$$\begin{aligned}W(k+1)&=W(k+1)-\mu\nabla J(k)\\&=W(k)-\mu\left\{\eta\frac{\partial e^2(k)}{\partial W}+(1-\eta)\frac{\partial(-\log(f(e(k))))}{\partial W}\right\}\end{aligned} \tag{7}$$

where $\nabla J(k)$ is the gradient of the integrated performance index $J(k)$ at time k, μ is the learning rate, which determines the convergence speed of the weight update algorithm.

In general, the PDF of the system error is unknown or is difficult to be obtained. In this paper, we use Parzen window nonparametric estimation approach [29] to estimate $f(e(k))$ of Eq. (7) in order to utilize the advantage of Renyi's quadratic entropy including all the information of random variable. Parzen window nonparametric estimation approach is a kernel

method that can estimate PDF from the system error. The estimated PDF of the error is expressed as

$$\hat{f}(e(k)) = \frac{1}{L}\sum_{i=k-L}^{k-1} \kappa_\sigma(e(k)-e(i)) \tag{8}$$

where $L>0$ denotes the window length, the selection of L depends on the length of the interval in which the signal of interest remains approximately stationary and the computational load limitation on each update. $\kappa_\sigma(\cdot)$ is the kernel function. For simplicity, we use the following kernel function:

$$\kappa_\sigma(x) = \frac{1}{\sqrt{2\pi}}\sigma\exp\left(-\frac{x^2}{2\sigma^2}\right) \tag{9}$$

where $\sigma>0$ is the kernel size, the selection of σ depends on the practical trial, which is critical to estimate Renyi's entropy. Moreover, Eq. (9) satisfies the following relation:

$$\kappa'_\sigma(x) = -x\sigma^{-2}\kappa_\sigma(x) \tag{10}$$

Substituting Eq. (8) into Eq. (7), and using Eqs. (1) and (3), we obtain the following generalized weight coefficient updating algorithm:

$$\begin{aligned} W(k+1) &= W(k)+\mu\left[2\eta e(k)\hat{X}(k)+(1-\eta)\frac{\sum_{i=k-L}^{k-1}\kappa'_\sigma(e(k)-e(i))(\nabla e(k)-\nabla e(i))}{\sum_{i=k-L}^{k-1}\kappa_\sigma(e(k)-e(i))}\right] \\ &= W(k)+\mu\left[2\eta e(k)\hat{X}(k)-(1-\eta)\frac{\sum_{i=k-L}^{k-1}(\hat{X}(k)-\hat{X}(i))\kappa'_\sigma(e(k)-e(i))}{\sum_{i=k-L}^{k-1}\kappa_\sigma(e(k)-e(i))}\right] \end{aligned} \tag{11}$$

where $\nabla e(k)$ is the instantaneous gradient of the system error $e(k)$, i.e., $\nabla e(k) = -s(k) * X(k) = -\hat{X}(k)$, $X(k)$ is the generalized input signal, $\hat{X}(k)$ is the generalized filtered-X signal, which is filtered through the secondary path model $S(z)$, $\hat{X}(k) = [\hat{X}'(k),\hat{X}'(k-1),\ldots,\hat{X}'(k-N+1)]^{\mathrm{T}}$, with $\hat{X}'(k-i) = [\hat{x}(k-i),\hat{x}^2(k-i),\ldots,\hat{x}^p(k-i)]^{\mathrm{T}}$, $i=0,1,\ldots,N-1$, $\hat{x}(k) = s(k) * x(k)$, and the operator $*$ denotes the linear convolution.

According to the proposed nonlinear neuro-controller with the GFX-IECGD algorithm, we can obtain the following nonlinear ANC system structure, which is illustrated in Fig. 3.

The secondary path transfer function $S(z)$ can be estimated by an additional FIR filter $\hat{S}(z)$ [1]. Therefore, the generalized filtered-X signal $\hat{X}(k)$ is generated by passing the reference signal through this estimate of the secondary path, $\hat{X}(k) = \hat{s}(k) * X(k)$, where $\hat{s}(k)$ is the estimated impulse response of the secondary path estimator $\hat{S}(z)$.

Remark 3. In this paper, the secondary path estimation is not considered in the design of control system, which is the normal case in ANC systems [6,7,11,14]. In fact, the secondary path includes some man-made instruments, e.g., a D/A converter, an amplifier, and an actuator, and their models can be precisely known. Therefore, we can assume that the secondary path is known through some off-line estimation methods. However, considering the fact that the secondary path may be time-varying if the environment is changed in some ways, an ANC method without the secondary path estimation needs to be further studied.

4. GFX-IECGD convergence analysis

Based on the updating law Eq. (11) for weights adjustment of the dynamic linear part in Fig. 2, the convergence analysis of the proposed algorithm is studied.

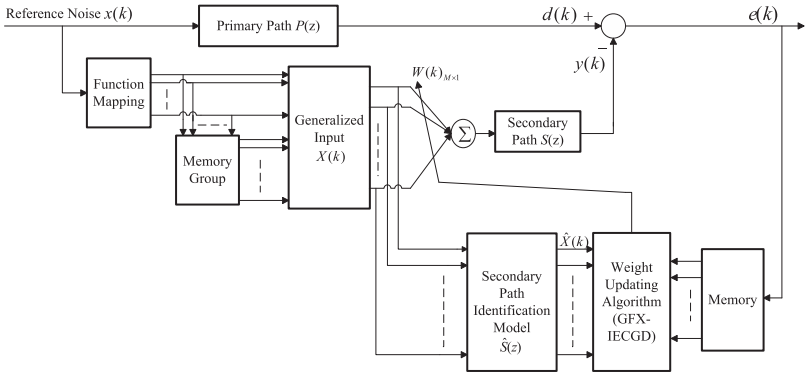

Fig. 3. Block diagram of nonlinear ANC system with the proposed scheme.

Suppose the optimal value of the generalized weight coefficient vector $W(k)$ of the dynamic linear part is W^*, and the primary noise $d(k)$ in Fig. 1 can be described as $d(k)=W^{*\mathrm{T}}\hat{X}(k)$ [17], then it is necessary that there exists an ideal control $u(k)$ to attenuate the primary noise $d(k)$.

Remark 4. For the convenience of the convergence analysis, the optimal weight vector W^* is only used to analyze the convergence of the proposed algorithm in this paper, but is not used in the practical implementation. In addition, by updating the weights $W(k)$ according to the weight coefficient adjustment law shown Eq. (11), $W(k)$ will finally converge to the optimal weight W^*.

Denote $\Delta W(k)$ as the gradient form of $J(k)$, we can rewrite Eq. (11) as

$$W(k+1)=W(k)-\mu\Delta W(k) \tag{12}$$

where

$$\Delta W(k)=-2\eta e(k)\hat{X}(k)+(1-\eta)\frac{\sum_{i=k-L}^{k-1}(\hat{X}(k)-\hat{X}(i))\kappa'_{\sigma}(e(k)-e(i))}{\sum_{i=k-L}^{k-1}\kappa_{\sigma}(e(k)-e(i))}$$

The error vector of the generalized weight coefficient vector $W(k)$ is defined as $\tilde{W}(k)=W(k)-W^*$, then subtracting W^* from both sides of Eq. (12) yields

$$\tilde{W}(k+1)=\tilde{W}(k)-\mu\Delta W(k) \tag{13}$$

Substituting $\tilde{W}(k)$ into Eq. (1), we obtain the following equation:

$$\begin{aligned} e(k)&=d(k)-y(k)=-(W(k)-W^*)^{\mathrm{T}}\hat{X}(k)\\ &=-\tilde{W}(k)^{\mathrm{T}}\hat{X}(k)=-\hat{X}(k)^{\mathrm{T}}\tilde{W}(k) \end{aligned} \tag{14}$$

Then substituting Eqs. (10), (12) and (14) into Eq. (13), we can obtain

$$\begin{aligned} \tilde{W}(k+1)&=\tilde{W}(k)-2\mu\eta R(k)\tilde{W}(k)+\mu(1-\eta)\left[\frac{\sum_{i=k-L}^{k-1}(\hat{X}(k)-\hat{X}(i))(e(k)-e(i))\kappa_{\sigma}(e(k)-e(i))}{\sigma^2\sum_{i=k-L}^{k-1}\kappa_{\sigma}(e(k)-e(i))}\right]\\ &=\tilde{W}(k)-2\mu\eta R(k)\tilde{W}(k)-\mu(1-\eta)\left[\frac{\sum_{i=k-L}^{k-1}(\hat{X}(k)-\hat{X}(i))(\hat{X}(k)-\hat{X}(i))^{\mathrm{T}}\tilde{W}(k)\kappa_{\sigma}(e(k)-e(i))}{\sigma^2\sum_{i=k-L}^{k-1}\kappa_{\sigma}(e(k)-e(i))}\right]\\ &=\tilde{W}(k)-2\mu\eta R(k)\tilde{W}(k)-\mu(1-\eta)\left[\frac{\sum_{i=k-L}^{k-1}\kappa_{\sigma}(e(k)-e(i))(\hat{X}(k)-\hat{X}(i))(\hat{X}(k)-\hat{X}(i))^{\mathrm{T}}}{\sigma^2\sum_{i=k-L}^{k-1}\kappa_{\sigma}(e(k)-e(i))}\tilde{W}(k)\right]\\ &=\tilde{W}(k)-2\mu\eta R(k)\tilde{W}(k)-2\mu(1-\eta)\Gamma(k)\tilde{W}(k) \end{aligned} \tag{15}$$

where

$$R(k)=\hat{X}(k)\hat{X}^{\mathrm{T}}(k),\ \kappa_{\sigma}(\cdot)\geq 0,\Gamma(k)=\frac{1}{2}\left[\frac{\sum_{i=k-L}^{k-1}\kappa_{\sigma}(e(k)-e(i))(\hat{X}(k)-\hat{X}(i))(\hat{X}(k)-\hat{X}(i))^{\mathrm{T}}}{\sigma^2\sum_{i=k-L}^{k-1}\kappa_{\sigma}(e(k)-e(i))}\right]$$

Considering that $(\hat{X}(k)-\hat{X}(i))(\hat{X}(k)-\hat{X}(i))^{\mathrm{T}}$ is non-negative, we have $\Gamma(k)\geq 0$. Then Eq. (15) can be rewritten as

$$\begin{aligned} \tilde{W}(k+1)&=\tilde{W}(k)-2\mu[\eta R(k)+(1-\eta)\Gamma(k)]\tilde{W}(k)\\ &=\tilde{W}(k)-\mu\Phi\tilde{W}(k) \end{aligned} \tag{16}$$

where $\Phi=2[\eta R(k)+(1-\eta)\Gamma(k)]$, $R(k)$ is the input vector correlation matrix and is assumed to be a symmetric positive definite matrix, thus the matrix Φ is positive definite.

According to the unitary similarity transformation method of matrix theory, the positive definite matrix Φ in the following Eq. (17) is diagonalized by unitary matrix Q:

$$\Phi=Q^{\mathrm{H}}\Lambda Q \tag{17}$$

where Λ is a diagonal matrix, in which the diagonal elements are the eigenvalues of matrix Φ. The unitary matrix Q satisfies $Q^{\mathrm{H}}Q=QQ^{\mathrm{H}}=I$, and $Q^{\mathrm{H}}=Q$. $V(k)=Q^{\mathrm{H}}\tilde{W}(k)$ is defined as the rotation transformation coefficient vector, $V(0)$ is set as the initial value, then Eq. (16) is rewritten as

$$QV(k+1)=(I-\mu\Phi)QV(k) \tag{18}$$

Left-multiplicating Q^{H} on both sides of Eq. (18), we obtain

$$V(k+1)=Q^{\mathrm{H}}(I-\mu Q^{\mathrm{H}}\Lambda Q)QV(k) \tag{19}$$

that is

$$\begin{aligned} V(k+1)&=(I-\mu\Lambda)V(k)\\ &=(I-\mu\Lambda)^{k+1}V(0) \end{aligned} \tag{20}$$

Then Eq. (20) can be written by

$$V(k+1)=\begin{bmatrix}(1-\mu\lambda_1)^{k+1} & 0 & \cdots & 0\\ 0 & (1-\mu\lambda_2)^{k+1} & \cdots & 0\\ \vdots & \vdots & \ddots & \vdots\\ 0 & 0 & \cdots & (1-\mu\lambda_{NP})^{k+1}\end{bmatrix}V(0) \tag{21}$$

where λ_i is the eigenvalue of matrix Φ.

In order to guarantee the convergence of the proposed algorithm, the absolute value of every elements of the matrix in Eq. (21) must be less than 1. Therefore, we can obtain the convergence condition of the proposed method as

$$0<\mu<1/\max\lambda_i,\quad i\in\{1,2,\ldots,NP\} \tag{22}$$

If the learning rate μ is chosen as $0<\mu<1/\max|\lambda_i|$, the convergence of the nonlinear neuro-controller with GFX-IECGD algorithm is guaranteed in the nonlinear ANC systems.

Under the condition equation (22), the generalized weight coefficient $W(k)$ will converge to the optimal value W^*. In this process, we describe the weight change process via a time constant. We can rewrite Eq. (20) as

$$\begin{aligned}v_i(k+1)&=(1-\mu\lambda_i)v_i(k)\\ &=(1-\mu\lambda_i)^{k+1}v_i(0)\end{aligned} \tag{23}$$

The error between the generalized weight coefficient and the optimal weight coefficient is transient, and the adaptive process approximates the exponential damping law. Suppose the unit time is equivalent to the time of one-iteration period, Eq. (23) denotes the ratio of two successive rotation transformation coefficient, which equals to $1-\mu\lambda_i$. Using the exponential change of time constant τ_i to represent the transient process, we obtain

$$1-\mu\lambda_i=\exp(-1/\tau_i)\approx 1-1/\tau_i,\mu\ll 1 \tag{24}$$

Thus, the time constant τ_i is described by the following equation:

$$\tau_i=\frac{-1}{\ln(1-\mu\lambda_i)}\approx 1/\mu\lambda_i \tag{25}$$

According to the above analysis, the learning rate μ should be chosen to fulfill Eq. (22).

Remark 5. According to Eq. (22), the convergence analysis presented above depends on the knowledge of the eigenvalues of matrix Φ, thus we will be able to determine the upper bound on the learning rate according to Eq. (22), which may be different under different noises. However, in general, a larger learning rate μ can improve the convergence rate and thus leads to a better adaptive process.

5. Computational complexity comparison

In order to show the efficiency of the proposed scheme, we analyze the computational complexity of the linear FIR filter with FXLMS algorithm [2], the nonlinear quadratic Volterra filter with Volterra FXLMS algorithm [8], and the nonlinear neuro-controller (NNC) with GFX-IECGD algorithm, respectively.

5.1. A FIR filter with FXLMS algorithm

The linear FIR filter with FXLMS algorithm [2] is applied to the ANC system, which has a similar structure as Fig. 1. The computational complexity per iteration of the FXLMS algorithm based linear FIR filter is analyzed as follows. This computation process requires three major operations.

(1) Calculate the FIR filter output $u(k)=W^{\mathrm{T}}(k)X(k)$, which requires N multiplications and $N-1$ additions. N denotes the length of the FIR filter, i.e., N is the dimension of the weight $W(k)$ and the input vector $X(k)$.
(2) Compute the filtered signal $\hat{x}(k)$ based on $\hat{x}(k)=\hat{s}(k)*x(k)$, which requires R multiplications and $R-1$ additions, where R denotes the length of the secondary path identification model $\hat{S}(z)$ estimated by a FIR filter.
(3) Update the filter weight coefficients by $W(k+1)=W(k)+2\mu\hat{X}(k)e(k)$, which requires $N+2$ multiplications and N additions.

Therefore, the ANC systems using the linear FIR filter need $2N+R+2$ multiplications and $2N+R-2$ additions.

5.2. A Volterra filter with VFXLMS algorithm

To reduce the computational complexity, only the quadratic Volterra filter can be used for real-time implementation. Therefore, the ANC system that uses a quadratic (second-order) Volterra filter with a Volterra FXLMS algorithm [8] is

analyzed, the structure of which is also similar as Fig. 1. As an example for a quadratic Volterra filter, the input vector is given as

$$X(k)=[x(k),\ldots,x(k-N+1),x^2(k),\ldots,x(k)x(k-N+1),\ x^2(k-1),\ldots,x(k-1)x(k-N+1),\ldots,x^2(k-N+1)]^{\mathrm{T}} \tag{26}$$

where N is the memory size of the quadratic Volterra filter, and the length of the weight coefficient vector of the quadratic Volterra filter is $N+N(N+1)/2=(N^2+3N)/2$. Similar to the linear FIR filter, this method also requires three major operations.

(1) Calculate the Volterra filter output $u(k)$, which requires $N(N+5)/2$ multiplications and $(N^2+3N-4)/2$ additions.
(2) Compute the filtered signal $\hat{x}(k)$, which requires R multiplications and $R-1$ additions, where $\hat{x}(k)=\hat{s}(k)*x(k)$.
(3) Update the filter weight coefficients, which requires N^2+2N+2 multiplications and $N(N+1)/2$ additions.

Therefore, the ANC systems using a second-order Volterra filter with a Volterra FXLMS algorithm need $(3N^2+9N+2R+2)/2$ multiplications and $N^2+2N+R-3$ additions.

5.3. NNC with GFX-IECGD algorithm

The nonlinear neuro-controller with the GFX-IECGD algorithm is applied to the ANC system shown in Fig. 3. Substituting Eq. (10) into Eq. (11), we obtain

$$W(k+1)=W(k)+2\mu\eta e(k)\hat{X}(k)+\mu(1-\eta)\frac{\sum_{i=k-L}^{k-1}(e(k)-e(i))\kappa_\sigma(e(k)-e(i))(\hat{X}(k)-\hat{X}(i))}{\sigma^2\sum_{i=k-L}^{k-1}\kappa_\sigma(e(k)-e(i))}. \tag{27}$$

The computational complexity per iteration is computed as follows.

(1) Calculate the controller output $u(k)$ given in Eq. (3), which requires NP multiplications and $NP-1$ additions.
(2) Compute the filtered signal $\hat{x}(k)$ given in the following equation $\hat{x}(k)=\hat{s}(k)*x(k)$, which requires R multiplications and $R-1$ additions.
(3) Update the filter weight coefficients, which requires $(L+1)(NP+1)+NP+6$ multiplications and $(NP+1)(2L+1)-1$ additions and L kernel function operations.

Therefore, ANC systems using the nonlinear neuro-controller (NNC) with GFX-IECGD algorithm needs $(L+1)(NP+1)+2NP+R+6$ multiplications, $2(NP+1)(L+1)+R-4$ additions and L kernel function operations. Specifically, by selecting $L=1$ and $P=2$ in Eq. (29), we simplify Eq. (27) to

$$W(k+1)=W(k)+2\mu\eta e(k)\hat{X}(k)+\mu(1-\eta)\sigma^{-2}\Delta e(k)\Delta\hat{X}(k) \tag{28}$$

where $\Delta e(k)=e(k)-e(k-1)$, $\Delta\hat{X}(k)=\hat{X}(k)-\hat{X}(k-1)$. Under this condition, the computational load needs $6N+R+7$ multiplications and $8N+R$ additions and 1 kernel function operations. When selecting $L=1$, $P=2$ and $\eta=0$, the computational load needs $4N+R+3$ multiplications and $6N+R-1$ additions.

In addition, when choosing $\eta=1$, we can rewrite Eq. (28) as

$$W(k+1)=W(k)+2\mu\hat{X}(k)e(k) \tag{29}$$

Eq. (29) describes a weight updating law, which can be defined as generalized filtered X least mean square (GFXLMS) algorithm. The GFXLMS algorithm is a special case of GFX-IECGD algorithm. When the proposed nonlinear neuro-controller with GFXLMS algorithm is used to the ANC system, the computational load needs $4N+R+2$ multiplications and $4N+R-2$ additions.

The computational load of the above control methods is summarized in Table 1. It is shown that the proposed nonlinear neuro-controller with $P=2$ has the obvious computational advantage over the second-order Volterra filter under the circumstance of using the LMS algorithm. In the special case, when the parameters of ANC using the proposed controller are selected as $P=2$, $L=1$, $\eta=0$, the GFX-IECGD algorithm has a similar structure and computational complexity with the

Table 1
Comparison of computational load.

Type of controller	Multiplication	Addition	Kernel operation
FIR, FXLMS	$2N+R+2$	$2N+R-2$	0
Second-order Volterra	$(3N^2+9N+2R+2)/2$	$N^2+2N+R-3$	0
NNC, GFXLMS ($P=2$)	$4N+R+1$	$4N+R-3$	0
NNC, GFX-IECGD ($P=2,L=1,\eta=0$)	$4N+R+3$	$6N+R-1$	1
NNC, GFX-IECGD ($P=2,L=1$)	$6N+R+7$	$8N+R$	1
NNC, GFX-IECGD	$(L+1)(NP+1)+2NP+R+6$	$2(NP+1)(L+1)+R-4$	L

GFXLMS algorithm. In fact, the GFX-IECGD algorithm under the condition of selecting $\eta = 0$ is equivalent to the algorithm based on Renyi's quadratic error entropy criterion. In addition, the computational complexity of the method with GFX-IECGD algorithm increases since the PDF of the system error is indirectly obtained by the Parzen window approach.

6. Simulation results

Extensive simulations for the nonlinear ANC system are conducted in this section. In the simulations, a sinusoidal narrowband noise with frequency 200 Hz and a logistic chaotic non-Gaussian broadband noise [6] are used to demonstrate the effectiveness of the proposed control scheme.

In practical ANC system, the secondary path exhibits non-minimum phase speciality besides that the primary path has the nonlinearity characteristic. In the simulations, the primary path model is selected as in [14]

$$d(k) = x(k-3) - 0.3x(k-4) + 0.2x(k-5) + 0.8x^2(k-5) \tag{30}$$

The secondary path model is selected as in [14]

$$y(k) = u(k-1) + 1.5u(k-2) - u(k-3) \tag{31}$$

Case 1: In this case, a sinusoidal noise with frequency 200 Hz is first utilized as a narrowband periodic noise, which is a non-Gaussian noise signal as shown in [20]. The sampling frequency is chosen to be 11 025 Hz. We compare the performances of two different approaches: the proposed nonlinear neuro-controller with GFX-IECGD algorithm (GFX-IECGD-NNC) and the adaptive Volterra filter based on FXLMS algorithm (VFX-LMS) [8]. We select a single neuron with 20 nodes and P=2, L=1, $\eta = 0.4$, $\sigma = 1$, $\mu = 0.07$ in the proposed nonlinear neuro-controller, and choose the learning rate $\mu = 0.003$ in the Volterra controller with second-order and the memory size N=5. Fig. 4 depicts the ANC system error under two different controllers. The result of the proposed GFX-IECGD-NNC is shown in the dashed line, and the result of the Volterra filter is shown in the solid line, and the detailed error is provided in Fig. 5.

Fig. 6 gives the simulation results of the canceling noises in the frequency domain. The solid line shows the power spectrum of active noise canceling error when the ANC system turns off, and the dotted line shows the power spectrum of active noise canceling error when the proposed method is applied. The dashed line shows the power spectrum of active noise canceling error under the condition of VFX-LMS approach.

From the results shown in Figs. 4 and 6, we can see that the proposed method can achieve a better performance although it provides a little sluggish transient at the beginning, and there exists a significant error shown in Fig. 5 under the condition of VFX-LMS approach. In Fig. 6, the power spectrum results demonstrate that the proposed method can attenuate the noises more greatly compared with the VFX-LMS approach.

Case 2: In this case, we use the proposed method for the same system as the first case, and the noise signal is the same as the case 1. We use a single neuron with M=40 nodes in the proposed controller, and the output signal of static memory function mapping is a pure quadratic serial, i.e., $X'(k) = [x(k), x^2(k)]$, the filtered-X signal $\hat{X}(k) = [x(k), x^2(k), x(k-1), \ldots, x^2(k-N+1)]$, and select L=10, $\eta = 0$, $\sigma = 1$, $\mu = 0.05$ and L=10, $\eta = 0.5$, $\sigma = 1$, $\mu = 0.007$, respectively, for two cases. In fact, If $\eta = 0$, the proposed method is simplified to the algorithm based on the pure Renyi's quadratic error entropy (RQEE) criterion. Fig. 7 shows the ANC system error under two different parameter conditions. Fig. 8 gives the simulation results of the canceling noises in the frequency domain. The solid line shows the power spectrum of active noise canceling error when the ANC system turns off, and the dashed line shows the power spectrum of active noise canceling error when the

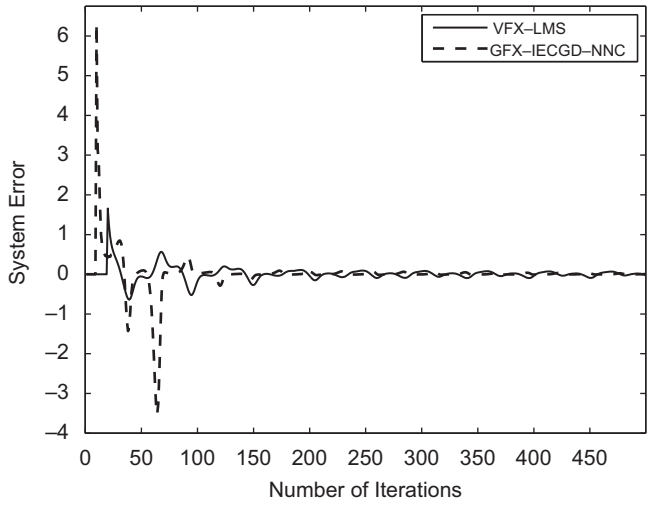

Fig. 4. The ANC system error.

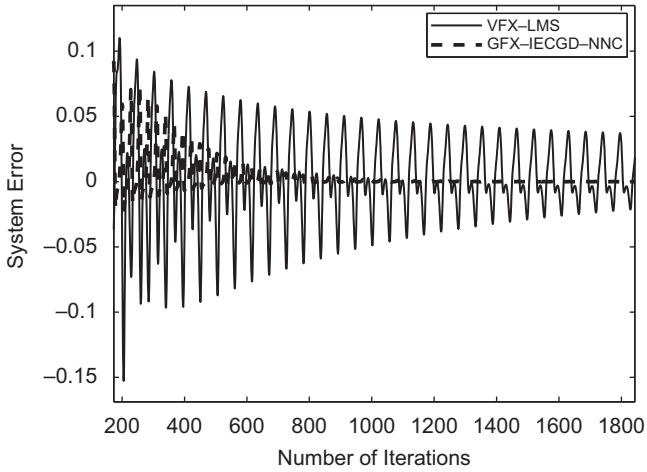

Fig. 5. Detail of the system error.

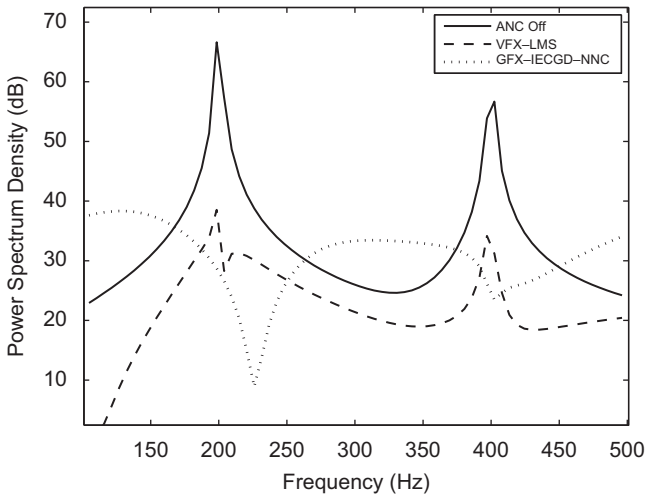

Fig. 6. Power spectrum of canceling errors.

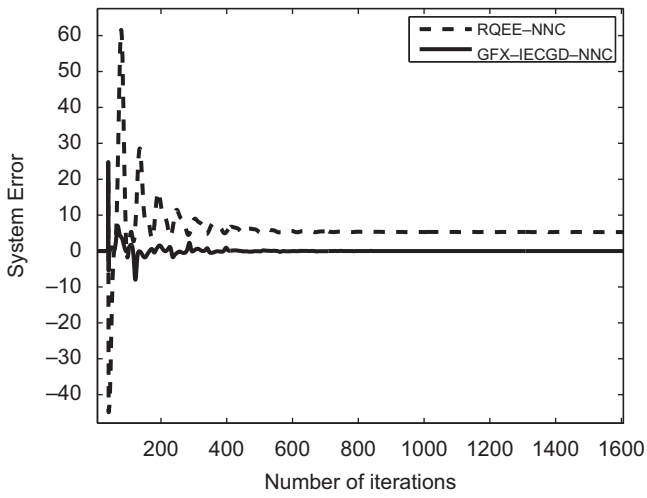

Fig. 7. The ANC system error.

proposed method is used under the condition of $\eta = 0$. The dotted line shows the power spectrum of active noise canceling error when the proposed method is used under the condition of $\eta = 0.5$.

From Fig. 7, it is obvious that there exists a significant system error when $\eta = 0$, but the system error tends to zero when $\eta = 0.5$. This is because Renyi's error entropy is only sensitive to the variation of the noises [17], ignores the mean information, which may result in a constant control error. However, the proposed integrated performance index can improve the system performance significantly. In Fig. 8, the power spectrum results demonstrate that the proposed method can greatly attenuate the nonlinear and non-Gaussian noises well while the proposed controller using the information entropy merely (e.g., RQEE criterion) cannot satisfy with the control demand. The above simulation results show that the integrated evaluation criterion has a better performance over the RQEE criterion.

Case 3: In this case, we use the same ANC system as case 1. The broadband noise signal is chosen to be a logistic chaotic signal [6], which is generated by the recursive equation $x(k+1) = \alpha x(k)[1-x(k)]$, where $\alpha = 4$ and $x(0)=0.9$ are chosen. This noise process is a non-Gaussian noise evaluated by its PDF distribution detection using the Matlab software. For the purpose of comparison, we implement the adaptive Volterra filter with FXLMS algorithm and the proposed nonlinear neuro-controller with GFX-IECGD algorithm. We select a single neuron with 20 nodes and $P=2$, $L=7$, $\eta = 0.35$, $\sigma = 1$, $\mu = 0.003$ in the proposed nonlinear neuro-controller, and choose the learning rate $\mu = 0.008$ in the Volterra controller with second-order and memory size $N=5$. Fig. 9 depicts the simulation results of each controller in the frequency domain. The solid line shows the power spectrum of active noise canceling error when the ANC system turns off, and the dotted line shows the power spectrum of active noise canceling error under the condition of VFX-LMS approach. The dashed line shows the power spectrum of active noise canceling error when the proposed method is applied. In Fig. 9,

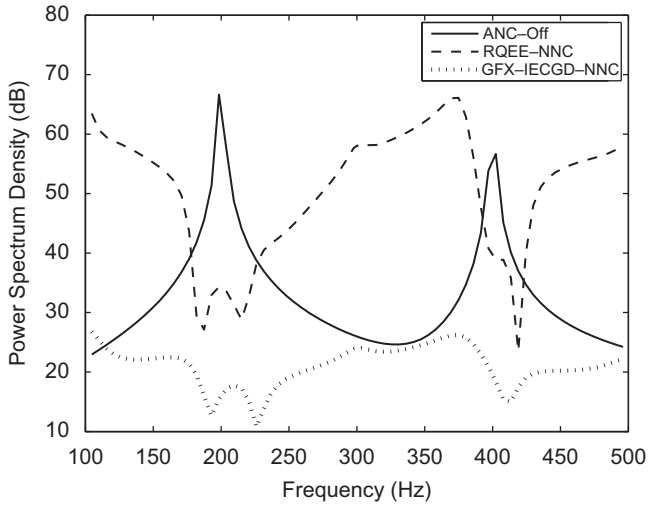

Fig. 8. Power spectrum of canceling errors.

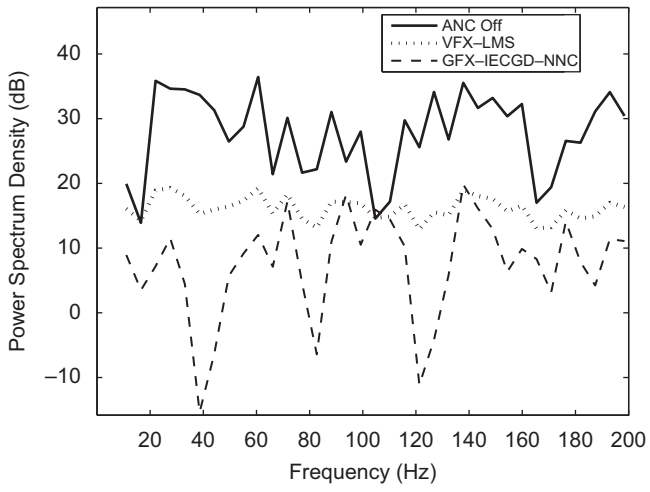

Fig. 9. Power spectrum of canceling errors for broadband noises.

it is seen that there is an improvement of performance of the NNC with GFX-IECGD algorithm over the Volterra filter with FXLMS algorithm.

The above simulations show that the proposed control scheme can attenuate the narrowband and broadband non-Gaussian noises in the nonlinear ANC systems. In addition, it is noted that the proposed control approach has a simple structure and less weights learning process, and can attenuate the non-Gaussian and nonlinear noises effectively.

7. Conclusions

In this paper, Renyi's entropy is introduced into active noise control systems to deal with the nonlinear and non-Gaussian noises. A nonlinear neuro-controller with a nonlinear memory function mapping is proposed for nonlinear ANC systems, and a generalized filtered-X algorithm based on an integrated evaluation criterion is utilized to update the control parameters on-line, which considers the respective advantage of information entropy and the mean square error. In addition, the convergence and computational complexity of the proposed method are analyzed. The presented control scheme has a simple control structure and less learning parameters. The effectiveness of the proposed approach is demonstrated by the simulation results.

References

[1] S.J. Elliott, *Signal Processing for Active Control*, Academic Press, London, 2001.
[2] S.M. Kuo, D.R. Morgan, Active noise control: a tutorial review, *Proceeding of IEEE* 87 (1999) 943–973.
[3] X. Sun, S.M. Kuo, M. Guang, Adaptive algorithm for active noise control of impulsive noise, *Journal of Sound and Vibration* 291 (2006) 516–522.
[4] R.S. Sanchez, M.A. Cuguero, A. Masip, J. Quevedo, V. Puig, Robust identification and feedback design: an active noise control case study, *Control Engineering Practice* 16 (2008) 1265–1274.
[5] M.T. Akhtara, W. Mitsuhashib, Improving performance of FxLMS algorithm for active noise control of impulsive noise, *Journal of Sound and Vibration* 327 (2009) 647–656.
[6] D.P. Das, G. Panda, Active mitigation of nonlinear noise processes using a novel filtered-s LMS algorithm, *IEEE Transactions on Speech and Audio Processing* 12 (2004) 313–322.
[7] D. Zhou, V. DeBrunner, Efficient adaptive nonlinear filters for nonlinear active noise control, *IEEE Transactions on Circuits and Systems: Regular Papers* 54 (2007) 669–681.
[8] L. Tan, J. Jiang, Adaptive Volterra filters for active control of nonlinear noise processes, *IEEE Transactions on Signal Processing* 49 (2001) 1667–1676.
[9] Y.L. Zhou, Q.Z. Zhang, X.D. Li, W.S. Gan, Analysis and DSP implementation of an ANC system using a filtered-error neural network, *Journal of Sound and Vibration* 285 (2005) 1–25.
[10] M. Bouchard, New recursive-least-squares algorithms for nonlinear active control of sound and vibration using neural networks, *IEEE Transactions on Neural Networks* 12 (2001) 135–147.
[11] C.Y. Chang, F.B. Luoh, Enhancement of active noise control using neural-based filtered-X algorithm, *Journal of Sound and Vibration* 305 (2007) 348–356.
[12] M.O. Tokhi, R. Wood, Active noise control using radial basis function networks, *Control Engineering Practice* 5 (1997) 1311–1322.
[13] S. Manikandan, M. Madheswaran, A new design of active noise feedforward control systems using delta rule algorithm, *Information Technology Journal* 6 (2007) 1162–1165.
[14] Q.Z. Zhang, W.S. Gan, Y.L. Zhou, Adaptive recurrent fuzzy neural networks for active noise control, *Journal of Sound and Vibration* 296 (2006) 935–948.
[15] H.Q. Zhao, X.P. Zeng, J.S. Zhang, Adaptive reduced feedback FLNN filter for active control of nonlinear noise processes, *Signal Processing* 90 (2010) 834–847.
[16] H. Yue, H. Wang, Minimum entropy control of closed-loop tracking errors for dynamics stochastic systems, *IEEE Transactions on Automatic Control* 48 (2003) 118–122.
[17] D. Erdogmus, Information Theoretic Learning: Renyi's Entropy and its Applications to Adaptive System Training, PhD Thesis, University of Florida, 2002.
[18] D. Erdogmus, K.E. Hild, J.C. Principe, Blind source separation using Renyi's-marginal entropy, *Neurocomputing* 49 (2002) 25–38.
[19] L. Guo, H. Wang, Minimum entropy filtering for multivariate stochastic system with non-Gaussian noises, *IEEE Transactions on Automatic Control* 51 (2007) 695–700.
[20] P. Afshar, H. Wang, ILC-based adaptive minimum entropy control for general stochastic systems using neural networks, *Proceedings of the 46th IEEE Conference on Decision and Control*, New Orleans, LA, USA, December 2008, pp. 252–257.
[21] D. Erdogmus, J.C. Principe, Convergence properties and data efficiency of the minimum error entropy criterion in adaline training, *IEEE Transactions on Signal Processing* 51 (2007) 1966–1978.
[22] B.D. Chen, J.C. Hu, Z.Q. Sun, A joint stochastic gradient algorithm and its application to system identification with RBF networks, *Proceedings of the 6th World Congress on Intelligent Control and Automation* (*WCICA*), Dalian, China, June 2006, pp. 1754–1758.
[23] V.J. Mathews, G.L. Sicuranza, *Sicuranza, Polynomial Signal Processing*, John Wiley & Sons Inc., New York, 2000.
[24] E.W. Bai, D. Li, Convergence of the iterative Hammerstein system identification algorithm, *IEEE Transactions on Automatic Control* 49 (2004) 1929–1940.
[25] G. Belforte, P. Gay, Discrete time Hammerstein model identification with unknown but bounded errors, *IET Proceedings Control Theory and Applications* 148 (2001) 523–529.
[26] M. Sznaier, Computational complexity analysis of set membership identification of Hammerstein and Wiener systems, *Automatica* 45 (2009) 701–705.
[27] X. Hong, R.J. Mitchell, Hammerstein model identification algorithm using Bezier–Bernstein approximation, *IET Control Theory and Applications* 1 (2007) 1149–1159.
[28] Y.B. Zhao, G.P. Liu, D. Rees, Networked predictive control systems based on the Hammerstein model, *IEEE Transactions on Circuits and Systems* 55 (2008) 469–473.
[29] E. Parzen, On the estimation of a probability density function and model, *Annals of Mathematical Statistics* 33 (1962) 1065–1076.
[30] Y.G. Niu, J. Lam, X.Y. Wang, D.W.C. Ho, Neural adaptive sliding model control for a class of nonlinear neutral delay systems, *Journal of Dynamic Systems, Measurement and Control* 130 (2008) 061011.